OsteoArthritis and Cartilage (2005) **13,** 896–905

doi:10.1016/j.joca.2005.05.003

Osteoarthritis and Cartilage

International Cartilage Repair Society

OARSI OSTEOARTHRITIS RESEARCH SOCIETY INTERNATIONAL

Development and remodeling of engineered cartilage-explant composites *in vitro* and *in vivo*[1]

Enrico Tognana Ph.D.†‡, Robert F. Padera M.D., Ph.D.†§, Fen Chen M.D.†, Gordana Vunjak-Novakovic Ph.D.† and Lisa E. Freed M.D., Ph.D.†*

† *Division of Health Sciences and Technology, Massachusetts Institute of Technology, Cambridge, MA, USA*

‡ *Fidia Advanced Biopolymers, Abano Terme, Italy*

§ *Department of Pathology, Brigham and Women's Hospital, Boston, MA, USA*

Summary

Objective: Development and remodeling of engineered cartilage-explant composites were studied *in vitro* and *in vivo*.

Design: Individual and interactive effects of cell chondrogenic potential (primary or fifth passage bovine calf chondrocytes), scaffold degradation rate (hyaluronan benzyl ester or polyglycolic acid), and adjacent tissue cell activity and architecture (vital trabecular bone (VB), articular cartilage (AC), devitalized bone (DB) or digested cartilage (DC)) were evaluated over 8 weeks *in vitro* (bioreactor cultures) and *in vivo* (ectopic implants).

Results: *In vitro*, significant effects of cell type on construct adhesive strength ($P < 0.001$) and scaffold type on adhesive strength ($P < 0.001$), modulus ($P = 0.014$), glycosaminoglycans (GAG) ($P < 0.001$), and collagen ($P = 0.039$) were observed. Chondrogenesis was best when the scaffold degradation rate matched the extracellular matrix deposition rate. *In vivo*, adjacent tissue type affected adhesive strength ($P < 0.001$), modulus ($P < 0.001$), and GAG ($P < 0.001$) such that 8-week values obtained for bone (VB and DB) were higher than for cartilage (AC). In the AC/construct group, chondrogenesis appeared attenuated in the region of the construct close to the AC. In contrast, in the VB/construct group, a 500 μm thick zone of mature hyaline-like cartilage formed at the interface, and signs of active remodeling were present in the bone that included osteoclastic and osteoblastic activity and trabecular rebuttressing; these features were not present in the DB group or *in vitro*.

Conclusions: Development and remodeling of composites based on engineered cartilage were mediated *in vitro* by cell chondrogenic potential and scaffold degradation rate, and *in vivo* by type of adjacent tissue and time.

Key words: Tissue engineered cartilage, Bone remodeling, Biomaterial, Bioreactor.

Introduction

Osteochondral defect repair remains an important, unsolved clinical problem, and a number of tissue engineering approaches involving cells and biomaterial scaffolds have been studied in an attempt to promote articular cartilage (AC) regeneration[1,2]. However, the most commonly used animal model, orthotopic implants in rabbit knee joints, is complicated by high variability and a fundamentally different biological situation from that existing in human joint lesions[2,3]. To address the problem of biological complexity, controlled *in vitro* studies have been done in petri dishes[4–7] and bioreactors[8,9]. Complementary *in vivo* data have also been obtained using ectopic (subcutaneous) implants in nude mice[10–15].

In the present study, *in vitro* (bioreactor) and *in vivo* (ectopic implant) models were utilized to explore the hypotheses that development and remodeling in composites made of engineered cartilage constructs and bone or cartilage explants depended on: (i) chondrogenic potential of the cell in the construct, (ii) scaffold degradation rate, (iii) adjacent tissue cell activity and architecture, and (iv) time (Fig. 1). We compared two cell types: primary (P0) calf chondrocytes that were expected to undergo rapid chondrogenesis[16,17] and fifth passage (P5) chondrocytes that were expected be dedifferentiated by serial expansion in monolayers using media containing 10% serum[18,19]. We compared two scaffolds: hyaluronan benzyl ester (Hyaff®11) that was expected to degrade only minimally over 8 weeks[9,20] and a structurally indistinguishable scaffold made of polyglycolic acid (PGA) that was expected to be almost completely degraded over 8 weeks[21,22].

We compared four different adjacent tissues: AC and vital trabecular bone, (VB), to represent the range of tissues involved in osteochondral defect repair[1], devitalized bone (DB) to explore whether bone cells or architecture influenced integration[9], and digested cartilage (DC) in an

[1]*Sources of support*: National Aeronautics & Space Administration (NNJ04HC72G; NCC8-174), Fidia Advanced Biopolymers (salary support of ET, materials & supplies).

Disclaimer: We attest that there was no conflict of interest, even though one of the scaffolds and a minor fraction of the funding were provided by Fidia Advanced Biopolymers.

*Address correspondence and reprint requests to: Dr Lisa E. Freed, M.I.T. E25-330, 77 Mass. Ave. Cambridge, MA, USA 02139. Tel: 1-617-253-3858; Fax: 1-617-258-8827; E-mail: Lfreed@mit.edu

Received 22 November 2004; revision accepted 4 May 2005.

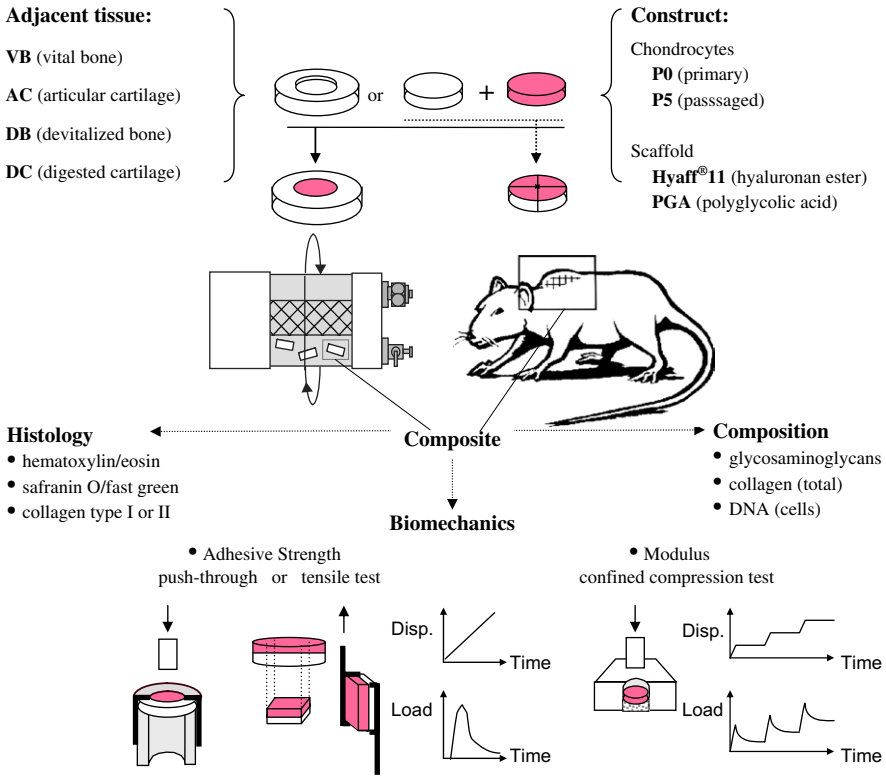

Fig. 1. Experimental design. Composites were generated using explanted adjacent tissues (VB, AC, DB, or DC) and constructs made of chondrocytes (P0 or P5) and biomaterial scaffolds (Hyaff®11 or PGA). Disc-in-ring composites made by press-fitting discs (5 × 2 mm) into rings (10/5 mm × 2 mm) were cultured in rotating bioreactors. Sandwich-like composites made by suturing together two discs (8 × 2 mm) were implanted subcutaneously in nude mice. Histology, biomechanics, and biochemical composition were evaluated after 4 and 8 weeks.

attempt to enhance integration by depletion of surface glycosaminoglycans (GAG)[8,23] in the explants. We evaluated composite histological structure, biomechanical properties, and biochemical composition after 4 and 8 weeks.

Methods

EXPERIMENTAL DESIGN

Twelve experimental groups were studied, each of which provided specific controls for other groups as follows. Based on our previous study[9], three basic groups were evaluated *in vitro* and *in vivo*; AC/P0/Hyaff®11, VB/P0/Hyaff®11, and DB/P0/Hyaff®11. *In vitro* we also studied AC/P5/Hyaff®11 composites, where dedifferentiated P5 cells provided a control for more chondrogenic P0 cells, and AC/P0/PGA composites, where quickly degrading PGA provided a control for more slowly degrading Hyaff®11. *In vitro* we also studied individually cultured specimens of VB and DB that, in contrast to AC[24], had not previously been cultured in rotating bioreactors. *In vivo*, we also studied DC/P0/Hyaff®11 composites, where DC was expected to provide a more adhesive substrate than AC[25] and VB/AC composites which provided an explant/explant control group.

CONSTRUCTS

Chondrocytes were obtained from full thickness cartilage harvested from the femoropatellar groove (FPG) of 2–4-week-old bovine calves within 8 h of slaughter[21]. The P0 cells were seeded onto scaffolds immediately after isolation, whereas the P5 cells were seeded onto scaffolds after five serial passages in monolayers plated at low initial density (10,000 cells/cm^2). All cells were cultured in Dulbecco's modified Eagle medium (DMEM) containing 4.5 g/L glucose, 10% fetal bovine serum (FBS), 10 mM 4-(2-hydroxyethyl)-1-piperazineethanesulfonic acid (HEPES) 0.1 mM nonessential amino acids, 0.4 mM proline, 50 mg/L L-ascorbic acid, 100 U/mL penicillin, 100 μg/mL streptomycin, and 0.5 μg/mL fungizone[21].

The Hyaff®11 and PGA scaffolds, respectively obtained from Fidia Advanced Biopolymers (Abano Terme, IT) and Smith & Nephew (York, UK), were formed as non-woven meshes that were indistinguishable with respect to three-dimensional structure[17]. The Hyaff®11 had a weight averaged molecular weight (M_w) of 168 kDa and was minimally degraded over 8 weeks[9,20,26], whereas the PGA had a M_w of 69 kDa and was essentially degraded over 8 weeks[22]. The scaffolds were wetted in FBS for 1–2 h, vacuum-dried, die-punched into discs, and seeded with cells for a period of 3 days in spinner flasks[9], using 60 million cells, 10 scaffolds (6 × 2 mm discs), and 150 mL per flask for *in vitro* studies, or 80 million cells, 10 scaffolds (8 × 2 mm discs), and 180 mL per flask for *in vivo* studies.

EXPLANTS

Osteochondral cores (10 and 8 mm in diameter for *in vitro* and *in vivo* studies, respectively) were obtained from the

FPG cartilage and subchondral trabecular bone of 2–4-week-old calves. A razor blade was first used to remove the uppermost 1 mm regions of cartilage (articular surface) or bone (subchondral plate), and then to make flat, 2 mm thick discs of AC or VB. To prepare DB type 2, discs of VB were extensively rinsed with distilled water (1 week) and lyophilized (3 days)[9]. To prepare DC, discs of AC were digested first for 16 h at 37°C in 0.01% (30 U/mL) collagenase type 2 (Worthington) containing 5% FBS in DMEM, then for 5 min at 37°C in 1 U/mL chondroitinase ABC (Seikagaku, Tokyo) in 10 mM Tris–HCl buffer[25]. Prior to composite preparation, AC discs were stored in DMEM for 24 h at 4°C, VB discs were cultured in DMEM for 16 h at 37°C, DB was stored dry at −20°C, and DC was rinsed and used immediately. Explants from a total of 24 different knee joints were used in six independent studies.

IN VITRO STUDIES

To make disc–ring composites, a construct disc (5 × 2 mm) was die-punched and press-fitted into a cartilage or bone ring (10/5 × 2–3 mm). After 7 days in orbitally mixed petri dishes, composites were placed in rotating bioreactors (RCCV 110, Synthecon, Houston) and maintained freely suspended by adjusting the rotation speed to 35–45 rpm[8,9]. Media were replaced two to three times per week and composites were sampled after 4 and 8 weeks. A total of 130 composites were cultured in a total of 13 bioreactors.

IN VIVO STUDIES

To make sandwich-like composites, a construct disc (8 × 2 mm) was sutured to a cartilage or bone disc (8 × 2–3 mm) using resorbable 5.0 Vicryl® (polyglycolide-co-lactide 90/10, Ethicon)[27]. The suture was wrapped around the two discs, knotted, wrapped around the composite in an orientation perpendicular to the first wrap, and again knotted. After 5–7 days in orbitally mixed petri dishes, composites were implanted in nude mice (National Institutes of Health (NIH) nu/nu, 8 week old, 25 g, Charles River) according to a protocol approved by an Animal Care and Use Committee. Anesthesia was induced and maintained using isofluorane (2–3%) and oxygen (1 L/min) supplied with a device made for rodents (IMPAC[6], VetEquip, Pleasanton) and administered by nasal cone. Composites were rinsed with phosphate buffered saline (PBS) and inserted into individual subcutaneous pouches, positioned such that the explant faced the dorsal musculature and the construct faced the skin. Composites were sampled after 3 days, 4 weeks, and 8 weeks. A total of 115 composites were implanted in 31 mice.

HISTOLOGICAL ANALYSES

Representative composites (two per data point) were fixed in 10% neutral buffered formalin for 24 h at room temperature (RT). Composites with AC or DC rings were transferred to 70% ethanol, whereas composites containing VB or DB rings were first decalcified using acidic decalcifier (RDO, Apex) and then placed in 70% ethanol[9]. Samples were embedded in paraffin, sectioned to 5 μm, stained with hematoxylin and eosin or safranin-O/fast green, and immunostained with monoclonal antibodies against bovine collagen types I and II[17].

BIOMECHANICAL ANALYSES

Representative composites (five to six per data point) were used to determine adhesive strength. First, fibrous surface capsules were removed in order to minimize artifacts[7]. Capsules were removed from *in vitro*-grown disc-in-ring composites by carefully shaving off the top and bottom surfaces using a microtome blade and specimen holding device[9]. The shaved sample was secured in a push-through device connected to a Electro-Force test system (ELF-3200, Bose, Framingham, MA) fitted with a 50 lb load cell, and compression (0.5 mm/min) was applied to the disc until it was displaced from the ring[9]. To facilitate capsule removal, we changed composite geometry for the subsequent *in vivo* studies, even though the change precluded direct comparison of adhesive strength data obtained *in vitro* and *in vivo*. The use of sandwich-like composites permitted efficient and reproducible preparation of a capsule-free composite by cutting an 8 mm diameter, 5–6 mm thick discoid sandwich into a 6 × 6 × 5–6 mm cuboid sandwich. The cuboid sandwich was secured in a custom-built testing device connected to an Instron (Model 5542, Canton, MA) fitted with a 500 N load cell, and tension (0.5 mm/min) was applied to one part of the device until it was displaced from a complementary part of the device. Each of the two complementary parts of the device had a square pocket (6 × 6 × 4 mm) into which the engineered construct or explanted tissue component of the sandwich could be secured. Spacers were inserted as needed below the construct and explant to align the interface of the sandwich with the interface of the device, which was made of highly polished aluminum to facilitate distraction. Data obtained from push-through and tensile tests were consistent with composite failure at the construct-tissue interface. In particular, load-displacement profiles showed a single, distinct peak after which the load decreased gradually to zero, consistent with interfacial fracture propagation[4] and complete removal of the surface capsule[7]. Construct adhesive strength was calculated as the measure of the ultimate load divided by the original overlap area.

Compressive modulus was assessed after adhesive strength testing, i.e., on constructs that appeared macroscopically intact but may have incurred molecular-level alterations. Constructs (five to six per data point) were equilibrated in PBS for 10 min at RT and placed in a chamber custom-designed to provide radial confinement while permitting uni-axial fluid flow via a stainless steel filter with 50 μm pore size. The chamber was filled with PBS and connected to the ELF-3200, using load cells of 250 g and 50 lb for *in vitro* and *in vivo* samples, respectively. Five consecutive stress-relaxations were applied: a 5% strain step followed by four 2% strain steps, each 600 s in duration. Constructs were considered to be fully relaxed during this increment based on a change in stress less than 0.009 MPa over the final 180 s. Data were recorded using a 10 Hz filter at an average sampling rate of 2 points/s. Equilibrium modulus was determined as the slope of the best linear regression fit ($r^2 > 0.95$) of equilibrium stress vs applied strain.

BIOCHEMICAL ANALYSES

Following biomechanical testing, constructs (four to six per data point) were weighed, frozen, lyophilized, and papain-digested[21]. The GAG content was measured spectrophotometrically using dimethylmethylene blue dye[28] and bovine chondroitin sulfate as a standard. Total collagen content was determined from the hydroxyproline content after acid

hydrolysis and reaction with *p*-dimethylaminobenzaldehyde and chloramine-T[29], using a hydroxyproline-to-collagen ratio of one-to-ten[30]. The cell content was calculated from DNA, assessed spectrofluorometrically with the use of Hoechst 33258 dye and conversion factors of 7.7 pg DNA per chondrocyte[31] and 10^{-10} g per chondrocyte[22].

STATISTICAL ANALYSIS

Statistical differences between groups was determined by multi-way analysis of variance (ANOVA) in conjunction with Tukey's *post hoc* test (Statistica Version 7, StatSoft, Tulsa, OK). *P*-values below 0.05 were considered statistically significant.

Results

IN VITRO STUDIES

Initial (3-day) constructs from all groups were comprised of scaffold fibers with attached cells ($0.50 \pm 0.06\%$ of wet weight, % ww), small amounts of GAG ($0.25 \pm 0.03\%$ ww), and low moduli (7 ± 1 kPa). Low moduli of initial constructs and structural instability of the non-woven meshes implied minimal contribution of the scaffold to final construct mechanical properties. Multi-way ANOVA showed a main effect of cell type on construct adhesive strength ($P < 0.001$) and interactive effects of cell type and time on adhesive strength ($P < 0.001$) and GAG content ($P < 0.001$) (Table I). The ANOVA also showed main effects of scaffold type on adhesive strength ($P < 0.001$), modulus ($P = 0.014$), GAG ($P < 0.001$), collagen ($P = 0.039$), and cells ($P < 0.001$) and interactive effects of scaffold type and time on GAG, collagen, and cells (Table I). As compared to corresponding constructs in the AC/P0/Hyaff®11 group, *post hoc* analysis showed that constructs made with P5 cells had lower GAG at 8 weeks, and that constructs made with PGA scaffolds had higher adhesive strength and GAG at 4 and 8 weeks (Table I).

In constructs cultured adjacent to AC, the extracellular matrix (ECM) of the construct did not project into the solid structure of the AC (Fig. 2). Constructs in the AC/P0/Hyaff®11 group were comprised of abundant scaffold remnants and tissue that was morphologically consistent with hyaline-like cartilage, i.e., round-to-oval chondrocytes in a matrix that stained positive for GAG [Fig. 2(A)] and collagen type II (not shown). In the AC/P5/Hyaff®11 group, constructs were comprised of scaffold remnants and fibrous tissue, i.e., actively dividing, spindle-shaped cells in a matrix that did not stain positive for GAG [Fig. 2(B)] or collagen type II, and instead stained for collagen type I (not shown). In the AC/P0/PGA group, minimal scaffold remnants were present and constructs were morphologically consistent with hyaline-like cartilage [Fig. 2(C, D)]. In all groups, a fibrous capsule, 100–300 μm thick comprising spindle-shaped cells and collagen type I, formed at the composite surfaces [Fig. 2(D)] as previously reported *in vitro*[7,9,24] and *in vivo*[11,12,21].

In constructs cultured adjacent to bone (VB and DB), the interface appeared interdigitated [Fig. 3(A, C)]. In the DB/construct group, chondrogenesis was evident at the interface and fibrous tissue filled the intertrabecular spaces [Fig. 3(A)], whereas individually cultured DB contained neither viable cells nor fibrous tissue [Fig. 3(B)]. The VB/construct group exhibited chondrogenesis at the interface [Fig. 3(C)], whereas individually cultured VB formed tissue resembling a periosteal bone collar at the inner diameter of the ring [Fig. 3(D)]. In VB rings cultured with and without constructs, a mixture of woven bone, hyaline-like cartilage, and fibrous tissue filled the intertrabecular spaces [Fig. 3(C, D)].

IN VIVO STUDIES

Multi-way ANOVA showed main effects of adjacent tissue type on construct adhesive strength ($P < 0.001$), modulus ($P < 0.001$), GAG ($P < 0.001$) and collagen ($P = 0.023$) (Table II). ANOVA also showed main effects of time on adhesive strength ($P = 0.032$), modulus ($P < 0.001$) and GAG ($P < 0.001$), consistent with previous reports[14,15], and interactive effects of adjacent tissue type and time (Table II). Constructs implanted for 8 weeks adjacent to bone (VB and DB) exhibited significantly higher adhesive strength, modulus, and GAG than corresponding constructs implanted adjacent to AC. Comparison of the VB/AC and VB/construct groups showed significantly higher adhesive strength in the latter group but significantly higher modulus, GAG, and collagen for AC than the construct (Table II). Comparison of average values obtained for the AC/P0/Hyaff®11 group *in vitro* and *in vivo* showed that the *in vivo* model yielded constructs with approximately five-fold higher moduli, two-fold higher GAG, and two-fold higher collagen (Table II vs Table I).

In the VB/AC group, composites exhibited a distinct interface, without any apparent integrative repair response by either component [Fig. 4(B)]. The intertrabecular bone spaces, which contained a mix of hematopoetic marrow elements, blood clots, and adipose tissue in 3-day explants [Fig. 4(A)], were filled mainly with adipose tissue by 4 weeks [Fig. 4(B)]. Fracture callus repair tissue was occasionally present in the VB, away from its interface with AC, and blood vessels were occasionally present in the immature calf cartilage and bone.

All constructs implanted adjacent to AC exhibited an asymmetric pattern of chondrogenesis wherein a mix of fibrocartilaginous tissue and densely packed scaffold remnants was present closer to the interface and more hyaline-like cartilage developed further from the interface with AC [Fig. 4(C, D)]. Enzymatic digestion yielded DC with a surface layer 150 μm thick that was devoid of GAG at the time of composite preparation, but was repleted with GAG after 4 and 8 weeks *in vivo* (not shown). Samples from the AC/construct and DC/construct groups exhibited comparable biomechanical and biochemical properties (Table II).

All constructs implanted adjacent to VB were comprised of hyaline-like cartilage [Fig. 5(A, B)]. Histology revealed a robust integrative repair response that included an interfacial region approximately 500 μm thick in which chondrocytes were aligned in columns [Fig. 5(A, B)]. Evidence of active bone resorption and formation included multinucleated osteoclasts degrading existing lamellar bone [Fig. 5(C)] and osteoblasts aligned on the surface of trabeculae in association with a distinctive cement line as new osteoid was deposited on pre-existing bone [Fig. 5(D, E)]. The intertrabecular spaces in the VB were filled with fracture callus repair tissue close to the interface, and adipose tissue elsewhere in explant. In the DB/construct group, trabecular remodeling was not observed, and construct and intertrabecular spaces were filled with a fibrocartilaginous tissue that stained positive for GAG [Fig. 5(F)].

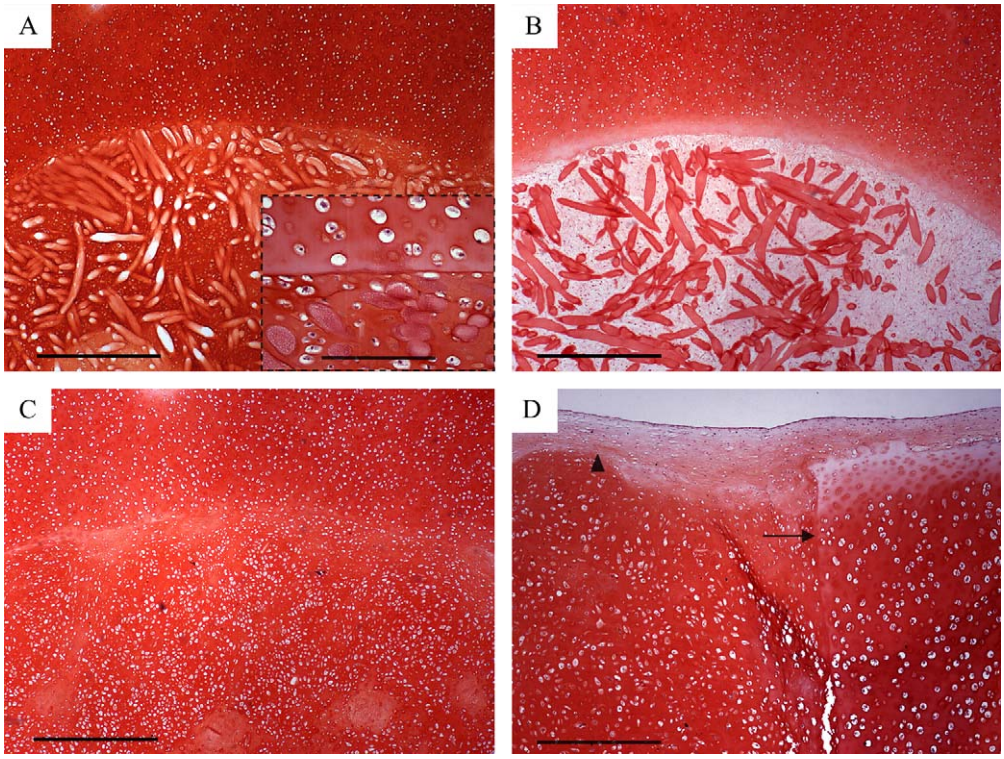

Fig. 2. *In vitro* effects of cellular chondrogenic potential and scaffold degradation rate. Histological appearance of 8-week samples of: (A) AC/P0/Hyaff®11, (B) AC/P5/Hyaff®11, and (C, D) AC/P0/PGA. Representative (A–C) transverse and (D) cross-sections stained with safranin-O/fast green. In (D), arrow points towards the AC region and arrowhead denotes fibrous capsule. Scale bars: (A–C) 500 μm, (D) 250 μm, Inset to (A) 100 μm.

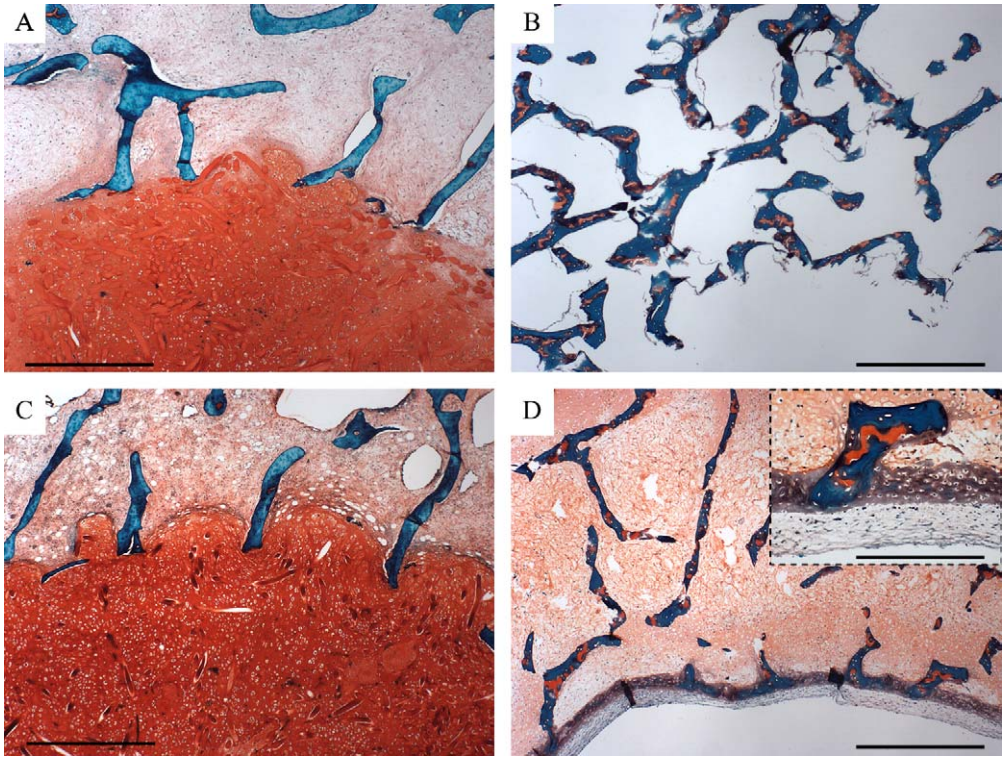

Fig. 3. *In vitro* effects of bone viability and construct presence. Histological appearance of 8-week samples of: (A) DB/P0/Hyaff®11, (B) DB, (C) VB/P0/Hyaff®11, and (D) VB. Representative sections stained with safranin-O/fast green. Scale bars: (A–D) 500 μm, Inset to (D) 200 μm.

Table I
Effects of type of cell and scaffold on the properties of constructs cultured in vitro

Property	Time (weeks)	Type of cell and scaffold			Main effect			Interactive effect	
		AC/P0/Hyaff	AC/P5/Hyaff	AC/P0/PGA	Cell type	Scaffold type	Time (t)	Cell × t	Scaffold × t
Adhesive Strength (kPa)	4	66.4 ± 26.9	255 ± 41*	153 ± 37.6†	$P < 0.001$	$P < 0.001$	NS	$P < 0.001$	NS
	8	134 ± 38.6	159 ± 45.2‡	267 ± 62.0†‡					
Modulus (kPa)	4	19.5 ± 7.93	16.2 ± 13.1	39.4 ± 19.2	NS	$P = 0.014$	NS	NS	NS
	8	30.9 ± 7.58	20.6 ± 7.10	48.5 ± 32.8					
GAG (% ww)	4	1.20 ± 0.23	1.64 ± 0.27	3.98 ± 0.71†	NS	$P < 0.001$	NS	$P < 0.001$	$P = 0.040$
	8	1.74 ± 0.27	0.38 ± 0.058*‡	3.88 ± 0.13†					
Collagen (% ww)	4	2.74 ± 0.53	3.56 ± 0.75	2.79 ± 0.59	NS	$P = 0.039$	NS	NS	$P = 0.016$
	8	2.36 ± 0.92	1.39 ± 0.42	4.98 ± 2.57†‡					
Cells (% ww)	4	0.911 ± 0.053	0.913 ± 0.325	0.843 ± 0.047	NS	$P < 0.001$	NS	NS	$P = 0.004$
	8	1.097 ± 0.071	0.972 ± 0.120	0.631 ± 0.039†					

Data are the average ± standard deviation of $n = 6$ mechanical or biochemical samples; NS, not significant.
*Significantly different from the corresponding sample made with P0 cells (AC/P0/Hyaff group).
†Significantly different from the corresponding sample made with Hyaff scaffold (AC/P0/Hyaff group).
‡Significantly different from the corresponding 4-week sample.

Table II
Effects of type of adjacent tissue and time on the properties of constructs implanted in vivo

Property	Time (weeks)	Type of adjacent tissue					Main effect		Interaction
		DC/construct	AC/construct	DB/construct	VB/construct	VB/AC	Adjacent tissue	Time (t)	Adjacent tissue × t
Adhesive strength (kPa)	4	176 ± 33	173 ± 52	413 ± 95*†	398 ± 33*†	134 ± 35‡			
	8	286 ± 84§	222 ± 62	509 ± 128*†§	334 ± 19†‖	196 ± 104‡	$P < 0.001$	$P = 0.032$	$P = 0.031$
Modulus (kPa)	4	100 ± 37	94 ± 21	142 ± 58	162 ± 59	739 ± 205‡			
	8	237 ± 93§	194 ± 53	360 ± 156*†§	637 ± 219*†§‖	961 ± 68‡	$P < 0.001$	$P < 0.001$	$P < 0.001$
GAG (% ww)	4	3.24 ± 0.35	2.63 ± 0.26	3.60 ± 0.14†	3.66 ± 0.47†	6.30 ± 0.36‡			
	8	3.75 ± 0.15§	3.81 ± 0.95	5.20 ± 0.91*†§	5.78 ± 1.16*†§	7.38 ± 0.92	$P < 0.001$	$P < 0.001$	NS
Collagen (% ww)	4	3.52 ± 1.26	4.04 ± 0.57	5.70 ± 0.79*	6.06 ± 1.38*	10.8 ± 1.84‡			
	8	4.10 ± 0.94	6.08 ± 2.02*§	4.13 ± 1.25	5.63 ± 0.58	9.52 ± 2.56‡	$P = 0.023$	NS	NS

Data are the average ± standard deviation of $n = 5$–6 mechanical or $n = 4$ biochemical analyses; NS, not significant.
*Significantly different from the corresponding DC sample.
†Significantly different from the corresponding AC sample.
‡Significantly different from the VB/construct group.
§Significantly different from the corresponding 4-week sample.
‖Significantly different from the corresponding DB sample.

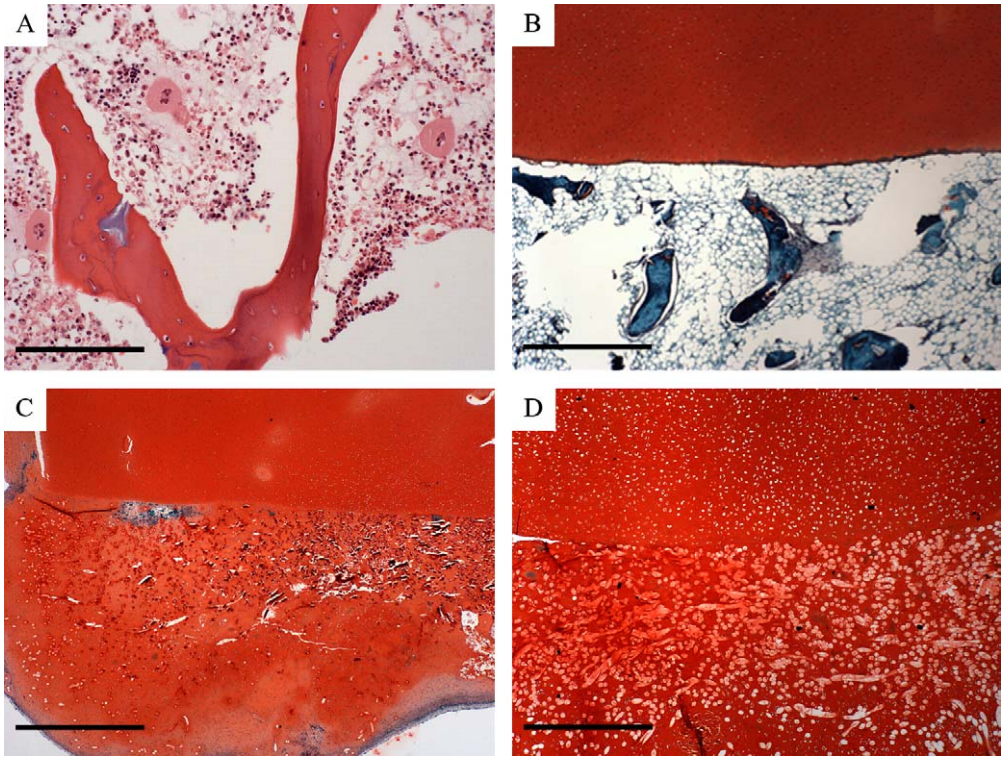

Fig. 4. *In vivo* effects of adjacent cartilage. Histological appearance of: (A) AC/VB at 3 days (bone region), (B) AC/VB at 4 weeks (interface), and (C, D) AC/P0/Hyaff®11 at (C) 4 weeks or (D) 8 weeks. Representative sections stained with (A) hematoxylin & eosin or (B–D) safranin-O/fast green. Scale bars: (A) 100 μm, (B, D) 500 μm, (C) 1.0 mm.

Discussion

Complementary *in vitro* and *in vivo* studies of development and remodeling in composites made of engineered cartilage and explanted cartilage or bone demonstrated significant effects of cell chondrogenic potential, scaffold degradation rate, adjacent tissue cell activity and architecture, and time. Our findings that constructs based on P5 cells exhibited fibrous histomorphology [Fig. 2(B)] and biomechanical and biochemical properties that deteriorated with time (Table I) can be attributed to cellular dedifferentiation, a process mediated by the animal species, donor age, cell density, and concentrations of serum and growth factors in the culture medium[32–35]. Our findings underscore the need to maintain and verify chondrogenic cell phenotype by coupling controlled expansion conditions with molecular-level assessment[18,19,36,37].

Our finding that rapidly degrading PGA scaffolds exhibited hyaline-like cartilage morphology [Fig. 2(C, D)] and relatively high GAG (Table I) can be explained by the good match between *in vitro* rates of scaffold degradation and cartilaginous ECM deposition by P0 calf chondrocytes cultured on PGA non-woven mesh in rotating bioreactors[16]. The importance of matching *in vivo* rates of scaffold degradation and osteochondral defect repair has also been demonstrated[38]. However, although rapidly degrading, polyester-based scaffolds yielded the best outcomes in bioreactors (Table I) and rabbits[38], more slowly degrading scaffolds may be required to match the slower rates of ECM deposition and defect repair in different models more relevant to human AC repair[13,38,39]. Our findings implied that rate of scaffold degradation was a critical variable, the appropriate selection of which in turn depended on the rates of cell- and tissue-level repair responses specific to the experimental model or clinical application.

In vivo, developmental chondrogenesis appeared attenuated in regions of the construct that were closely apposed to cartilage explant [Fig. 4(C)], and adhesive strength, modulus, and GAG were all significantly lower in the AC/construct group than in either of the bone/construct groups (Table II). Moreover, VB/AC composites exhibited no integrative response from either component [Fig. 4(B)], whereas VB/construct composites exhibited robust interfacial remodeling [Fig. 5(A–E)]. Together, these data implied that the presence of adjacent AC negatively affected construct development and integrative repair *in vivo*. Adverse effects of AC were not abolished by depletion of surface GAG using a modification of an enzymatic technique previously shown improve cell adhesion to AC[25]. Further studies are warranted to develop methods that may improve integration by depleting specific AC components, as previously discussed[40–43].

Interestingly, in the VB/construct group we observed repair responses similar in some respects to the fracture callus repair tissue that forms during the healing of a fractured bone[44], including a wide central zone of cartilaginous tissue comprising chondrocytes aligned in columns [Fig. 5(A, B)] and rebuttressing of the trabeculae by new bone formation on the pre-existing bone [Fig. 5(D, E)]. The above responses were present only in the VB group *in vivo*, and not the DB group *in vivo* [Fig. 5(F)], the VB group *in vitro* [Fig. 3(C)], or the DB group *in vitro* [Fig. 3(A)]. Our findings implied that the presence of adjacent VB, a rich source of soluble factors involved in chondrogenesis[45] and

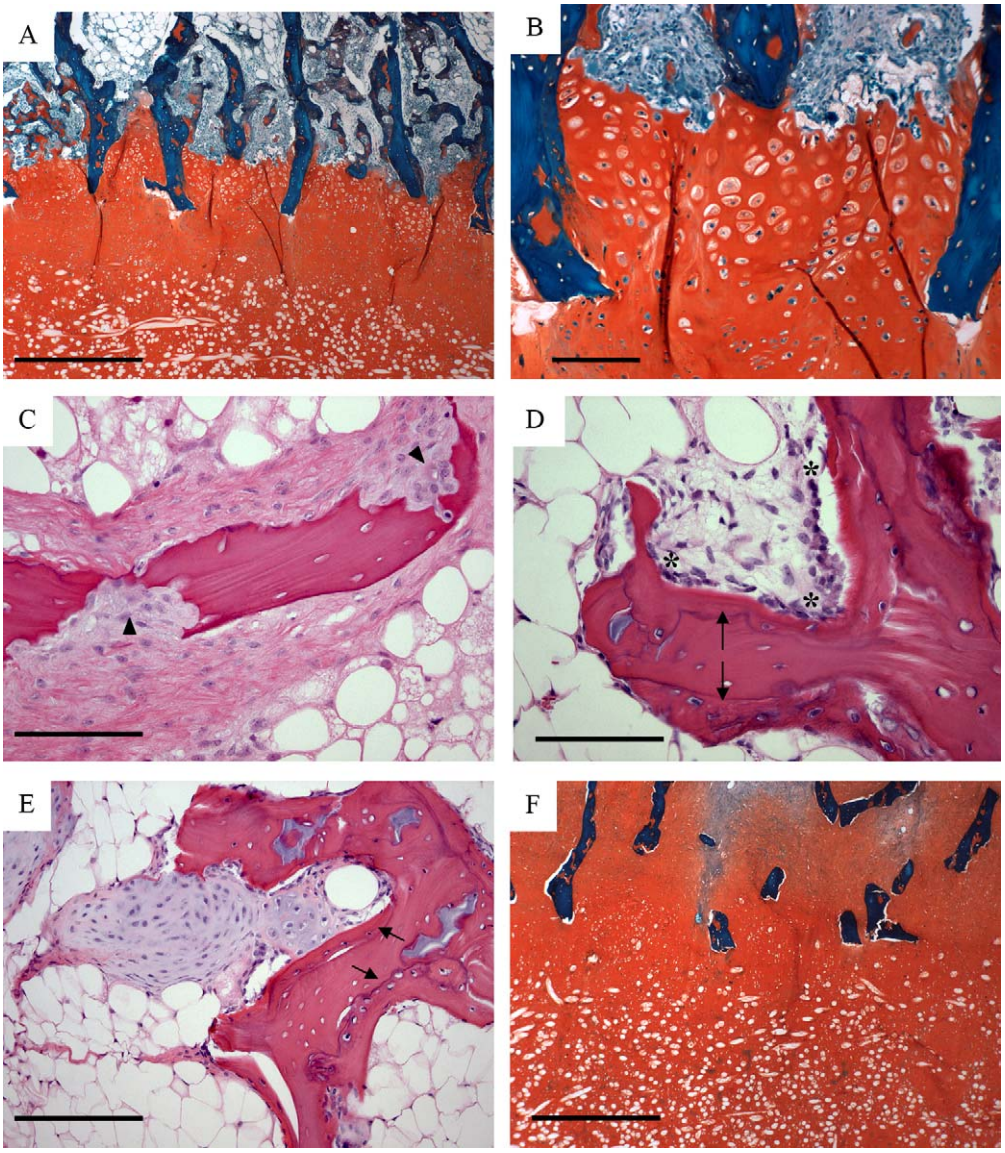

Fig. 5. *In vivo* effects of adjacent bone. Histological appearance of (A, B, D, E) VB/P0-Hyaff®11 at 8 weeks, (C) VB/P0/Hyaff®11 at 4 weeks, and (F) DB/P0/Hyaff®11 at 8 weeks. Representative sections stained with (A, B, F) safranin-O/fast green or (C–E) hematoxylin & eosin. In (C) arrowheads denote osteoclasts; in (D) asterisks denote osteoblasts, in (D, E) arrows point to cement lines (trabecular rebuttressing). Scale bars: (A, F) 500 μm; (B–E) 100 μm.

the remodeling of cartilage[46,47] and bone[44,48] positively affected integrative repair *in vivo*. The data also contribute to a growing body of literature addressing the bone–cartilage interface in osteochondral tissues, a transitional region critically important to joint structure and function[1].

In the present study, rotating bioreactor and ectopic implant models provided complementary data to that which can be obtained in more complex orthotopic implant models. Our findings that construct properties (e.g., moduli, GAG) were higher *in vivo* than *in vitro* and that certain histological features (e.g., chondrocyte alignment, bone remodeling) were observed only *in vivo* may be explained by differences between the two models including presence and concentration of oxygen and biophysical regulatory factors, mass transport, and mechanical environment. Together, the data demonstrate that it may be useful to study the development and remodeling of engineered cartilage via coordinated studies carried out *in vivo*, i.e., an environment providing a variable mix of host-derived regulatory factors, and *in vitro*, i.e., a more controlled setting in which one or several factors can be systematically studied.

Acknowledgments

This study was funded by the National Aeronautics and Space Administration (Grants NCC8-174 and NNJ04HC72G) and Fidia Advanced Biopolymers (Sponsored Research Agreement). We thank D. LaVan, M. Stading, and I. Martin and F. Guilak for help with biomechanics, H. Leddy and M. Radisic for help with statistics, R. Langer for general advice, and S. Kangiser for help with manuscript preparation.

References

1. Lynn AK, Brooks RA, Bonfield W, Rushton N. Repair of defects in articular joints. Prospects for material-based solutions in tissue engineering. J Bone Joint Surg Br 2004;86:1093–9.
2. Hunziker EB. Articular cartilage repair: basic science and clinical progress. A review of the current status and prospects. Osteoarthritis Cartilage 2001;10:432–63.
3. Hunziker EB. Biologic repair of articular cartilage. Defect models in experimental animals and matrix requirements. Clin Orthop 1999;367S:S135–46.
4. Reindel ES, Ayroso AM, Chen AC, Chun DM, Schinagl RM, Sah RL. Integrative repair of articular cartilage *in vitro*: adhesive strength of the interface region. J Orthop Res 1995;13:751–60.
5. DiMicco MA, Sah RL. Integrative cartilage repair: adhesive strength correlates with collagen deposition. J Orthop Res 2001;19:1105–12.
6. DiMicco MA, Waters SN, Akeson WH, Sah RL. Integrative articular cartilage repair: dependence on developmental stage and collagen metabolism. Osteoarthritis Cartilage 2002;10:218–25.
7. Moretti M, Wendt D, Schaefer D, Jakob M, Hunziker EB, Heberer M, *et al.* Structural characterization and reliable biomechanical assessment of integrative cartilage repair. J Biomech, in press.
8. Obradovic B, Martin I, Padera RF, Treppo S, Freed LE, Vunjak-Novakovic G. Integration of engineered cartilage. J Orthop Res 2001;19:1089–97.
9. Tognana E, Chen F, Padera RF, Leddy HA, Christensen SE, Guilak F. *et al.* Adjacent tissue (cartilage, bone) affect the functional integration of engineered calf cartilage *in vitro*. Osteoarthritis Cartilage 2005;13: 129–38.
10. Lipman JM, McDevitt CA, Sokoloff L. Xenografts of articular chondrocytes in the nude mouse. Calcif Tissue Int 1983;35:767–72.
11. Peretti GM, Randolph MA, Caruso EM, Rossetti F, Azaleske DJ. Bonding of cartilage matrices with cultured chondrocytes: an experimental model. J Orthop Res 1998;16:89–95.
12. Peretti GM, Bonassar LJ, Caruso EM, Randolph MA, Trahan CA, Zaleske DJ. Biomechanical analysis of a chondrocyte-based repair model of articular cartilage. Tissue Eng 1999;5:317–26.
13. Kafienah W, Jakob M, Demarteau O, Frazer A, Barker MD, Martin I, *et al*. Three-dimensional tissue engineering of hyaline cartilage: comparison of adult nasal and articular chondrocytes. Tissue Eng 2002;8:817–26.
14. Peretti GM, Zaporojan V, Spangenberg KM, Randolph MA, Fellers J, Bonassar LJ. Cell-based bonding of articular cartilage: an extended study. J Biomed Mater Res 2003;64A:517–24.
15. Randolph MA, Villa M, Peretti GM, Bonassar LJ, Yaremchuk MJ. Mechanics of tissue engineered cartilage integration to bone. Trans Orthop Res Soc 2004;29: paper 0041.
16. Freed LE, Hollander AP, Martin I, Barry JR, Langer R, Vunjak-Novakovic G. Chondrogenesis in a cell-polymer-bioreactor system. Exp Cell Res 1998;240:58–65.
17. Pei M, Solchaga LA, Seidel J, Zeng L, Vunjak-Novakovic G, Caplan AI, *et al*. Bioreactors mediate the effectiveness of tissue engineering scaffolds. FASEB J 2002;16:1691–4.
18. Schulze-Tanzil G, Mobasheri A, de Souza P, John T, Shakibaei M. Loss of chondrogenic potential in dedifferentiated chondrocytes correlates with deficient Shc-Erk interaction and apoptosis. Osteoarthritis Cartilage 2004;12:448–58.
19. Martin I, Vunjak-Novakovic G, Yang J, Langer R, Freed LE. Mammalian chondrocytes expanded in the presence of fibroblast growth factor-2 maintain the ability to differentiate and regenerate three-dimensional cartilaginous tissue. Exp Cell Res 1999;253:681–8.
20. Campoccia D, Doherty P, Radice M, Brun P, Abatangelo G, Williams DF. Semisynthetic resorbable materials from hyaluronan esterification. Biomaterials 1998; 19:2101–27.
21. Freed LE, Marquis JC, Nohria A, Emmanual J, Mikos AG, Langer R. Neocartilage formation *in vitro* and *in vivo* using cells cultured on synthetic biodegradable polymers. J Biomed Mater Res 1993;27:11–23.
22. Freed LE, Vunjak-Novakovic G, Biron R, Eagles D, Lesnoy D, Barlow S, *et al*. Biodegradable polymer scaffolds for tissue engineering. Biotechnology 1994; 12:689–93.
23. Hunziker EB, Kapfinger E. Removal of proteoglycans from the surface of defects in articular cartilage transiently enhances coverage by repair cells. J Bone Joint Surg Br 1998;80B:144–50.
24. Vunjak-Novakovic G, Obradovic B, Martin I, Freed LE. Bioreactor studies of native and tissue engineered cartilage. Biorheology 2002;39:259–68.
25. Lee MC, Sung KL, Kurtis MS, Akeson WH, Sah RL. Adhesive force of chondrocytes to cartilage. Effects of chondroitinase ABC. Clin Orthop 2000;Jan:286–94.
26. Milella E, Brescia E, Massaro C, Ramires PA, Miglietta MR, Fiori V, *et al*. Physico-chemical properties and degradability of non-woven hyaluronan benzylic esters as tissue engineering scaffolds. Biomaterials 2002;23: 1053–63.
27. Benicewicz BC, Hopper PK. Polymers for absorbable surgical sutures – Part I. J Bioactive Compatible Polym 1990;5:453–72.
28. Farndale RW, Buttler DJ, Barrett AJ. Improved quantitation and discrimination of sulphated glycosaminoglycans by the use of dimethylmethylene blue. Biochim Biophys Acta 1986;883:173–7.
29. Woessner JF. The determination of hydroxyproline in tissue and protein samples containing small proportions of this imino acid. Archiv Biochem Biophys 1961; 93:440–7.
30. Hollander AP, Heathfield TF, Webber C, Iwata Y, Bourne R, Rorabeck C, *et al*. Increased damage to type II collagen in osteoarthritic articular cartilage detected by a new immunoassay. J Clin Invest 1994; 93:1722–32.
31. Kim YJ, Sah RL, Doong JYH, Grodzinsky AJ. Fluorometric assay of DNA in cartilage explants using Hoechst 33258. Anal Biochem 1988;174:168–76.
32. von der Mark K, Gauss V, von der Mark H, Muller P. Relationship between cell shape and type of collagen synthesised as chondrocytes lose their cartilage phenotype in culture. Nature 1977;267:531–2.
33. Benya PD, Shaffer JD. Dedifferentiated chondrocytes reexpress the differentiated collagen phenotype when cultured in agarose gels. Cell 1982;30:215–24.
34. Malpeli M, Randazzo N, Cancedda R, Dozin B. Serum-free growth medium sustains commitment of human articular chondrocyte through maintenance of Sox9 expression. Tissue Eng 2004;10:145–55.
35. Mandl EW, van der Veen SW, Verhaar JA, van Osch GJ. Multiplication of human chondrocytes with low

seeding densities accelerates cell yield without losing redifferentiation capacity. Tissue Eng 2004;10: 109–18.
36. Jakob M, Demarteau O, Schaefer D, Hintermann B, Dick W, Heberer M. *et al*. Specific growth factors during the expansion and redifferentiation of adult human articular chondrocytes enhance chondrogenesis and cartilaginous tissue formation *in vitro*. J Cell Biochem 2001;81:368–77.
37. Grigolo B, Lisignoli G, Piacentini A, Fiorini M, Gobbi P, Mazzotti G, *et al*. Evidence for redifferentiation of human chondrocytes grown on a hyaluronan-based biomaterial (HYAff 11): molecular, immunohistochemical and ultrastructural analysis. Biomaterials 2002;23: 1187–95.
38. Solchaga LA, Temenoff JS, Gao J, Mikos AG, Caplan AI, Goldberg VM. Repair of osteochondral defects with hyaluronan- and polyester-based scaffolds. Osteoarthritis Cartilage 2005;13:297–309.
39. Meinel L, Hofmann S, Karageorgiou V, Zichner L, Langer R, Kaplan D, *et al*. Engineering cartilage-like tissue using human mesenchymal stem cells and silk protein scaffolds. Biotechnol Bioeng 2004;88: 379–91.
40. Caplan AI, Elyaderani M, Mochizuki Y, Wakitani S, Goldberg VM. Principles of cartilage repair and regeneration. Clin Orthop 1997;342:254–69.
41. Giurea A, DiMicco MA, Akeson WH, Sah RL. Development-associated differences in integrative cartilage repair: roles of biosynthesis and matrix. J Orthop Res 2002;20:1274–81.
42. Bos PK, DeGroot J, Budde M, Verhaar JA, van Osch GJ. Specific enzymatic treatment of bovine and human articular cartilage: implications for integrative cartilage repair. Arthritis Rheum 2002;46:976–85.
43. van de Breevaart Bravenboer J, In der Maur CD, Bos PK, van Rensen IH, Weinans H, Feenstra L, *et al*. Increased interfacial strength of transplanted cartilage *in vivo* following enzymatic treatment of wound edges. Trans Orthop Res Soc 2003;28: paper 0188.
44. Gerstenfeld LC, Cullinane DM, Barnes GL, Graves DT, Einhorn TA. Fracture healing as a post-natal developmental process: molecular, spatial, and temporal aspects of its regulation. J Cell Biochem 2003;88: 873–84.
45. Tuan RS. Cellular signaling in developmental chondrogenesis: N-cadherin, Wnts, and BMP-2. J Bone Joint Surg Am 2003;85-A(Suppl 2):137–41.
46. Luyten FP, Yu YM, Yanagishita M, Vukicevic S, Hammonds RG, Reddi AH. Natural bovine osteogenin and recombinant human bone morphogenetic protein-2B are equipotent in the maintenance of proteoglycans in bovine articular cartilage explant cultures. J Biol Chem 1992;267:3691–5.
47. Sellers RS, Zhang R, Glasson SS, Kim HD, Peluso D, D'Augusta DA, *et al*. Repair of articular cartilage defects one year after treatment with recombinant human bone morphogenetic protein-2 (rhBMP-2). J Bone Joint Surg Am 2000;82:151–60.
48. Yoo JU, Johnstone B. The role of osteochondral progenitor cells in fracture repair. Clin Orthop 1998; S73–81.